Spring 2020

Tidal-Groundwater Study of the Slaughter Beach Salt Marsh in Slaughter Beach, DE

Michael Powers
mp920214@wcupa.edu

Tidal-Groundwater Study of the Slaughter Beach Salt Marsh in Slaughter Beach, Delaware

A Thesis

Presented to the Faculty of the

Department of Geology and Astronomy

West Chester University

West Chester, Pennsylvania

In Partial Fulfillment of the Requirements for

the Degree of

Master of Science

By

Michael Powers

May 2020

Dedication

I dedicate this work to my late father, Richard Ernest Powers; a dedicated father, and a courageous man. His firm resolve, quiet strength, and determination made me the scientist and man I am today.

Acknowledgements

I would like to thank the College of Sciences and Mathematics and the Earth and Space Sciences Department for their generous grant funding. These grants enabled our research team to purchase groundwater equipment, receive UAS license training, transportation and lodging for our field work.

I would also like to thank my research advisor, Dr. Daria Nikitina for her dedication, patience, and mentorship throughout this project and my graduate career; Dr. Helmke, for providing valuable hydrogeologic expertise; Dr. Lutz, for creating manageable data sets and analysis programs; Dr. Bosbyshell, for graduate advisement, and Joan Kaiser for coordinating supply orders and grant funds.

Lastly, I would like to thank my fellow students, Alan Geyer and Michael Cohen; for technical skills training, Cameron Knight; for data analysis, and Magnus Payzine and Katie Dowling; for field work assistance.

Abstract

Seasonal and decadal monitoring of salt marsh at Slaughter Beach, DE documented long-term and short-term variations in number and sizes of salt ponds. Over 400 salt ponds ranging in size between 0.5 m^2 to 0.11 km^2 were identified on 5.5 km^2 salt marsh platform. The purpose of this study is to quantify hydrologic conditions and measure groundwater discharge of a salt marsh, particularly the impact of tidal forces on groundwater fluctuation.

Four wells with nests of mini-piezometers with ONSET Pressure Transducers were installed along a transect crossing the largest salt pond (0.11 km^2) in the study area. Nests of wells, installed at depths of 1 m, 3 m, and 6 m recorded groundwater hydraulic head at five-minute intervals during a 90 day period. High resolution aerial imagery of the studied ponds was collected at peak high tide and low tide using an unmanned aerial system. Changes in groundwater elevation were correlated with tidal data recorded by the USGS stream gauge in Cedar Creek.

Our results document the presence of 2 aquifers; deep (3m) and shallow (1m). Relationship between groundwater elevation and tidal fluctuations is strong in the deep aquifer and weak in the shallow aquifer. Analysis of drone imagery reveal no changes in the shape or size of the pond during 1 tidal cycle. Groundwater elevation decreases in proportion to distance from Cedar Creek and decreases with depth. We suggest that the deep aquifer is confined. This study has established a baseline for hydrologic investigations within the salt marsh.

Table of Contents

List of Tables

List of Figures

Introduction

Estuarine salt marshes provide a wide variety of ecosystem services. Coastal and estuarine communities rely on salt marsh ecosystems for protection from storm surges and coastal erosion (Barbier et al., 2011). Salt marshes absorb wave energy through stabilizing sediment with marsh grass roots and uptake extra water during high tides (Morgan et al, 2009). Salt marsh ecosystems are full of diverse flora and fauna. Many different species of fish, crustaceans, insects and waterfowl live and reproduce in these estuarine wetlands. Estuarine salt marshes also act as a coastal ocean filter. Salt marshes intercept large concentrations of nitrates from agricultural runoff before it enters the ocean (Nelson, 2012). In addition to storing nitrates, estuarine salt marshes effectively sequester large amounts of carbon in salt marsh plants by shifting the carbon cycle from a short-term cycle to a long-term cycle in the form of buried peat (Mayor and Hicks, 2008). The services that are provided by estuarine salt marshes makes them economically important areas to monitor and study.

The estuarine salt marshes of Delaware Bay have been around ~2000 years, since the late Holocene (Nikitina, 2015). Salt marshes develop on flat, coastal surfaces under conditions enabling a slow rate of sea level rise and sediment buildup, where the influx of sediments is higher than the erosion of the salt marsh platform (Townend et al, 2011). Estuarine salt marshes of Delaware Bay are at risk of inundation due to acceleration of sea level rise. The nearest tidal station in Lewes, Delaware, recorded a trend of 3.53 mm/year with a 95% confidence interval of +/- 0.23mm/year, based on 100 years of monthly sea level data (Figure 1). This is equivalent to a change of 0.35 meters over the past century (NOAA, 2020). The effects of sea level rise acceleration on estuarine salt marshes include erosion and salt marsh inundation (Reed, 1995).

Development of salt ponds on the marsh surface has been identified as one of the mechanisms of salt marsh inundation (Mariotti, 2016).

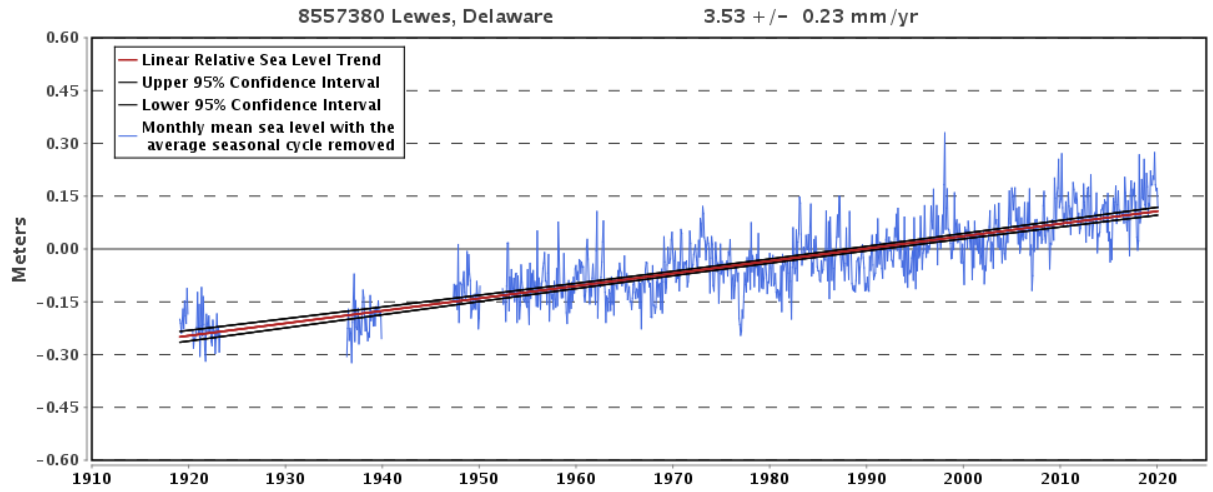

Figure 1: Relative sea level trend from 1917 to 2020 at tidal station 8557380 in Lewes, DE.

Salt ponds are shallow depressions of unvegetated surface filled in with saline water (Mariotti, 2016). Salt ponds may form tidal flats that become surrounded by vegetation (primary origin), or they may form due to disturbances in the existing marsh vegetation (secondary origin) (Wilson et al, 2009). However, the mechanisms by which the salt ponds form and how they develop is still poorly understood.

Recent study of the Slaughter Beach salt marsh has documented over 1400 ponds ranging from $0.5m^2$ to $0.11km^2$ in size (Geyer, et al, 2018). The number of ponds has been changing seasonally and following storm events. Changes in salt pond size, circularity, and distribution have been observed after large storm events, such as hurricanes (Irene/Sandy). Seasonal observation of salt pond changes has shown progressive development of salt ponds from November 2017 to September 2018 (Cohen et al, 2019). Therefore, these landforms are dynamic

as they change their size and shape over time. Sustained inundation and salt pond development could be an indicator of the resiliency of the marsh to continued sea level rise.

In addition to rising sea level, the Slaughter Beach salt marsh has been modified by humans. Historical dredging of Delaware Bay, ditching of the salt marsh, and jetty construction have directly impacted sediment fluxes and tidal flow to the salt marsh platform. The human impact on sediment supply and hydrologic regime of the marshes certainly contributed to changes of the salt marsh landscape and needed to be explored further in the effort of ecosystem conservation.

Further understanding of the hydrologic interactions between surface water and groundwater is also needed to assess the vulnerability of the salt marsh platform.

While the surface hydrology of the Slaughter Beach salt marsh has been monitored through historical and aerial drone imagery (Geyer, et al, 2018), little is known about the groundwater dynamics. Groundwater maps developed for the state of Delaware are too general to capture the localized groundwater flow active in the Slaughter Beach salt marsh.

The purpose of this study is to establish and quantify hydrologic conditions operating on a salt marsh, particularly the effect of tidal forces on saline groundwater fluctuation. Results of this study will create a baseline for hydrogeologic conditions active in the Slaughter Beach salt marsh.

Study Area

The Slaughter Beach salt marsh is located directly west of the town of Slaughter Beach, Delaware, on the southeast side of Delaware Bay (Figure 2). The study area covers approximately 5.5km^2 of salt marsh platform, between Slaughter Beach and Cedar Creek. The

marsh landscape includes tidal creeks, mosquito ditches, Cedar Creek channel, salt ponds and a wooded highland known as Sheppard's Island. Most of the Delaware estuarine salt marshes, including Slaughter Beach marsh, are vegetated by *Sp. Alterniflora*, *Sp. Patens*, and *Distichlis Spicata* species of salt-marsh grasses. (Nikitina, 2014). Salt marsh surface is subdivided into the high marsh and low marsh floral zones based on elevation and duration of tidal inundation. High marsh zones are at slightly higher elevations on the relatively flat marsh surface, and experience less tidal influx of sediment and saline water, which promotes the growth of *Sp. Patens* and *Distichlis Spicata*, which are less saline tolerant. Low marsh zones; located near salt ponds, tidal channels, and mosquito ditches, experience sustained periods of tidal flooding and are dominated by *Sp. Alterniflora* species of marsh grasses (Silvestri et al, 2005).

The Slaughter Beach salt marsh is underlain by the St. Marys formation, the uppermost formation of the Chesapeake Group (Ramsey, 1997). The late-Miocene age St. Marys formation is defined by bluish-gray silt with fine quartz sand and some shell beds. Overlying the Chesapeake Group is the Pleistocene Columbia Formation, described as a light reddish brown to white, cross-bedded medium to coarse sand with scattered thin beds of pebbles and gravel. The Columbia formation can range from 0 – 80ft in thickness across the state of Delaware.

The regional aquifer identified in the Slaughter Beach salt marsh area is the surficial Columbia aquifer (Kasper, 2017). The Columbia aquifer occurs predominantly in Pleistocene to Pliocene age sediments of the Columbia Formation.

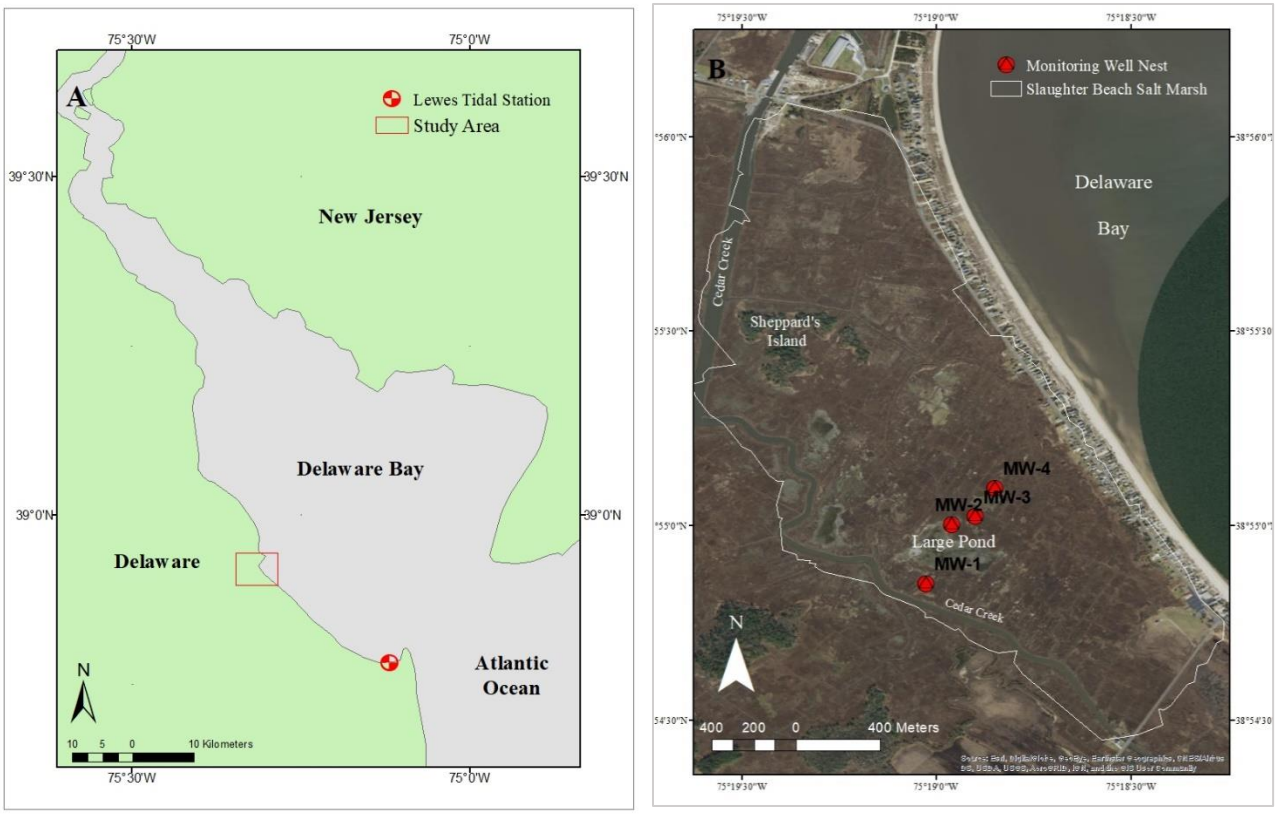

Figure 2: A: Map of study area on the coast of Delaware. B: Detailed map of the Slaughter Beach salt marsh.

The Slaughter Beach salt marsh has been modified by humans for 150 years or so. According to Beers Atlas (1868), the study area was drained by Cedar Creek, which flowed across the marsh into Delaware Bay (Figure 3). Over 150 years Cedar Creek has been altered by dredging, widening, and construction of a jetty at the mouth (Smith, 1988). A channel was cut from Cedar Creek extending North to the Mispillion River in 1869, preventing Cedar Creek from emptying into Delaware Bay through the Slaughter Beach salt marsh (Scharf, 1888). During the 1930's, the Slaughter Beach salt marsh was significantly changed by digging a network of mosquito ditching in order to control mosquito populations (Bourn and Cottam, 1950). Over time, some of those ditches have widened, some of turned into tidal creeks, and some have merged with salt ponds.

Figure 3: Modification of Cedar Creek into a man-made channel. Original course of Cedar Creek documented in Beers Atlas (1868), georeferenced to the WGS84 Geodetic Datum. Georeferencing and analysis provided by Cameron Knight.

Salt pond development on the Slaughter Beach salt marsh surface has been the focus of recent studies. Between 1400 to 1500 salt ponds ranging in size from $0.03m^2$ to $73,477m^2$ were documented within the Slaughter Beach salt marsh (Cohen et. al, 2019). In order to conduct a more detailed analysis of salt pond morphology, we selected a small study area ~ $0.15km^2$ around the largest pond at the Slaughter Beach salt marsh (Figure 4) and collected drone imagery for ~ 10 months (November 2017 to September 2018) to monitor seasonal changes and tidal influence of the ponds of various sizes. During the observation period, the total number of ponds changed from 26 ponds to 414 ponds within the immediate area around the largest pond. Of the $0.15km^2$ area, salt ponds made up approximately 31% of the marsh surface (Figure 3). Most of the ponds are no larger than $10m^2$ in surface area.

Stratigraphy below the salt ponds indicated that most of the ponds in the study area are developed during the last several hundred years, or at least not at the same time as the salt marsh began to develop in the study area (Cohen et al., 2019).

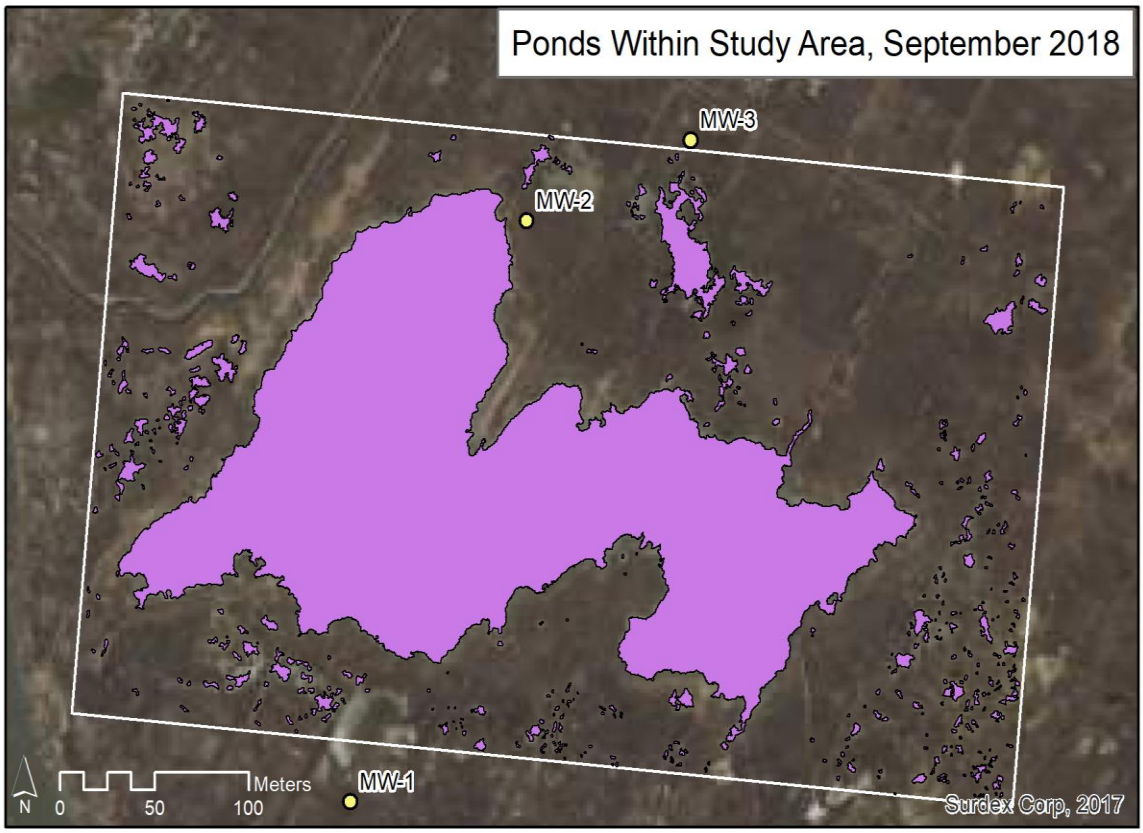

Figure 4: Study area (0.15km^2) includes the largest pond on the Slaughter Beach salt marsh. Imagery provided by Cameron Knight.

Methods

Well Installation and Stratigraphic Investigation

The largest pond on the surface was chosen as the focus of this tidal-groundwater study (Figure 4). A transect passing through the large pond, as well as two other adjacent ponds, was set (Figure 5). Eleven sediment cores were collected along the transect to document the stratigraphy and sediment characteristics. Cores were collected using a 5cm diameter Eijelkamp auger. Sediments were described in the field by visual inspection of color, amount of organic matter and grain sizes. Based on stratigraphy and proximity to ponds, four piezometer nests were installed along the transect in the Summer of 2019 (Figure 4). Piezometers were constructed

using 1.5-meter lengths of 2.5cm diameter Schedule 40 PVC. The screened section of the well casing is slotted at 10mm intervals. Well boreholes were cored using a 10cm diameter Eijelkamp auger. Boreholes were cored in 1m increments. Well boreholes were lined with #1/20 Uniform Packing Sand. The top of the borehole was packed with B-20 Mesh Granular Bentonite to ensure a tight seal. Piezometer nests MW-1 and MW-2 contained three wells, installed to depths of ~1m, 3m and 5m. Piezometer nests MW-3 and MW-4 each contained two wells, installed to depths of ~1m and 3m (Table 1).

Figure 5: Detailed map of study area, showing locations of piezometer nests and sediment core locations used to construct the stratigraphic cross section.

	Nest-1			***Nest-2***			***Nest-3***		***Nest-4***	
Well ID	*MW-1S*	*MW-1D*	*MW-1DD*	*MW-2S*	*MW-2D*	*MW-2DD*	*MW-3S*	*MW-3D*	*MW-4S*	*MW-4D*
Lat./Long.	38.9142 N 75.31712 W	38.9142 N 75.31712 W	38.9142 N 75.31712 W	38.91672 N 75.31604 W	38.91672 N 75.31604 W	38.91672 N 75.31604 W	38.91707 N 75.31504 W	38.91707 N 75.31504 W	38.91828 N 75.31419 W	38.91828 N 75.31419 W
Well Elevation (cm)	202.110	202.103	202.467	202.194	202.260	202.543	202.368	202.486	202.319	202.278
Borehole Depth (cm)	100	300	500	100	300	500	100	300	100	300
Casing Depth (cm)	96.01	243.84	361.20	86.40	230.80	353.20	75.40	217.80	76.40	243.84
Transducer Depth (cm)	100	298	425	145	292	424	150	294	135	292

Table 1: Well Dimensions. Well elevation was measured from top of casing and referenced to NAVD88 Geodetic Datum.

Well surface elevation was measured using a Sokkia SET530R Total Survey Station. In order to reference well elevation to a common datum, a temporal survey benchmark was set up using an Emlid Reach RS+ GPS survey system. Its elevation was measured using real-time kinematic (RTK) satellite positioning and referenced to the NAVD88 Vertical Geodetic Datum. The nearest United States Geodetic Survey benchmark, HU0180, was found to be inaccessible.

ONSET Pressure transducers were installed within each piezometer at 90% of the depth of the well, connected with steel cable to locking plugs at the top of the well casing. One transducer was set above the water level to record barometric pressure for data correction. The transducers were each set to record the water column length at 5-minute intervals. A bail-down slug test was conducted at each piezometer. Approximately 0.25 liters was bailed from each piezometer. The rising hydraulic head was recorded by the transducer in each well. The transducers continued to record the water level in each well from May 15, 2019 to July 27, 2019.

Collected transducer data was used to construct the equipotential lines of groundwater flow in the stratigraphic cross section. Groundwater elevation values recorded for the peak of the Spring Tide at 9:57 PM on June 3rd, 2019. Equipotential lines were drawn on the cross section with a contour interval of 20 centimeters.

Drone Imagery Collection

In order to document the influence of tidal fluctuations on pond size, aerial photographs with a spatial resolution of 2in. per pixel were captured using a Zenmuse X3 EO Gimbal Camera mounted on a DJI Inspire 1 Unmanned Aerial System (drone) at high and low tides. The imagery collection flights were conducted on June 2nd, 2019 at 8:58 AM to capture peak high tide, and 2:52 PM for peak low tide. Flight paths were acquired using Drone Deploy and DJI Go software

that calculated the transect flights required to collect imagery of the study area. The drone flew both flights at an altitude of 400 feet above sea level. Approximately 175 images were captured over a surface area of ~0.11 km^2. Drone Deploy used photogrammetry to process the collected images and convert them into geoTIFF files. Both flights were referenced to the WGS84 Datum.

Adobe Photoshop software was used to identify and digitize salt ponds on the collected imagery from both flights. The boundaries of the large pond and surrounding smaller ponds were delineated and their areas quantified. Quantitative comparison between the data collected at high and low tide were performed to establish relationship between pond size and tidal cycle.

Hydrologic Data Processing

Pressure transducers were collected from the piezometers in August 2019. Data recorded on the ONSET pressure transducers was downloaded into a .csv format. Transducer data was corrected for barometric pressure through HOBOware groundwater software. Total hydraulic head was calculated from depth to water subtracted from the surveyed well elevation.

Tidal data was collected from the USGS Stream Gauge 01484235 in Cedar Creek, that covered the duration of the study period (USGS, 2019). All data was normalized in the NAVD88 Vertical Datum. The tidal station records water levels at 6-minute intervals, therefore, groundwater data from the study area was normalized into a similar time base. Once a similar time base was established, tidal data and groundwater observation data were plotted on a time series chart.

Precipitation data was collected for the study period from May 2019 through July 2019 from the Delaware Environmental Observing System weather station (DEOS, 2019). Data was only available for June 2019 and July 2019, due to damage that occurred to the station in May.

Significant precipitation events were plotted on the same time series chart with the groundwater observation data.

Groundwater observation data was analyzed through the Hvorslev Method for Bail-down Slug Tests (Hvorslev, 1951). Prior to installing the pressure transducer in the piezometer, static water level was recorded and then the piezometer was purged. The recharge from the purged water level back to the static water level was recorded by the transducer. The Hvorslev Method normalizes each recorded water level of recharge into a fraction of the total drawdown (Table 2). Calculated values were plotted over time taken to recharge to static water level (Figure 6).

Depth to Water (cm)	**Drawdown *s* (cm)**	s/s_{max}	**Elapsed Time (minutes)**
223.9031	49.25272	1	1
222.9278	48.27736	0.980197	5
221.8305	47.18008	0.957918	10
219.8798	45.22936	0.918312	15
218.813	44.16256	0.896652	20
217.6547	43.00432	0.873136	25
216.405	41.75464	0.847763	30

Table 2: Detailing the process of creating the Hvorslev Drawdown curve for MW-1D. Maximum drawdown (s_{max}) was divided into each drawdown measurement until the initial static water level was reached. Static water level for MW-1D was recorded as 174.76cm DTW.

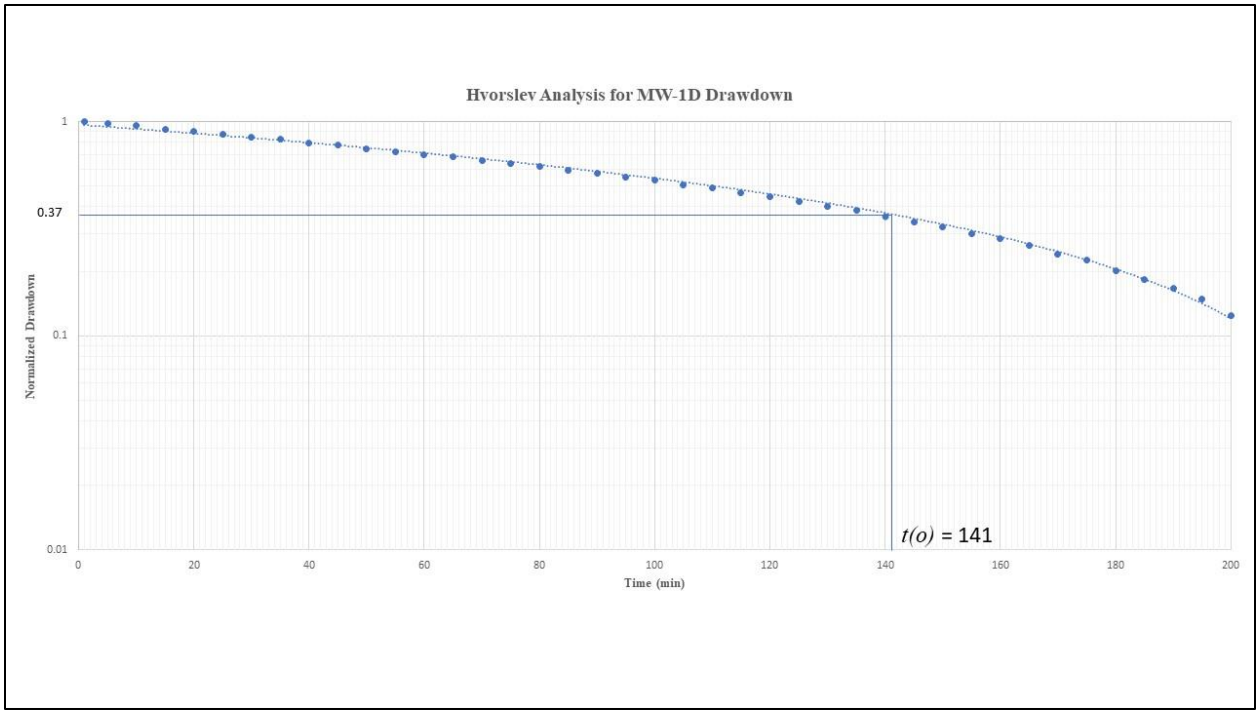

Figure 6: Hvorslev Drawdown curve for MW-1D. The curve was used to find point t_0, to determine the hydraulic conductivity of the well.

Hydraulic conductivity (K) was calculated for each piezometer using the Hvorslev Slug Test Solution (Equation 1).

(Equation 1) $$K = \frac{r^2 \ln\left(\frac{L}{R}\right)}{2Lt_0}$$

Where (K) is the hydraulic conductivity, (r) is the screen radius, (R) is the radius of the well casing, (L) is the length of the screened interval, and (t_0) is determined from the Hvorslev drawdown curve (Figure 6).

Due to the tidal influence of nearby Cedar Creek, the Jacob's Tidal Method was found to be the method to determine diffusivity (Jacob, 1950). Diffusivity was calculated (Equation 2) for

each piezometer based on a co-series chart detailing tidal amplitude and groundwater fluctuation on May 27, 2019 (Figure 7).

(Equation 2) $$D = \frac{\pi x^2}{t_0[\ln(\frac{h_0}{h_x})]^2}$$

Where (D) is hydraulic diffusivity, (x) is distance from nearest tidal source, (h_0) is the tidal amplitude during one complete tidal cycle, (h_x) is the head fluctuation within the well during the same tidal cycle, and (t_0) is the time lag between the peak of high tide to the peak of hydraulic head.

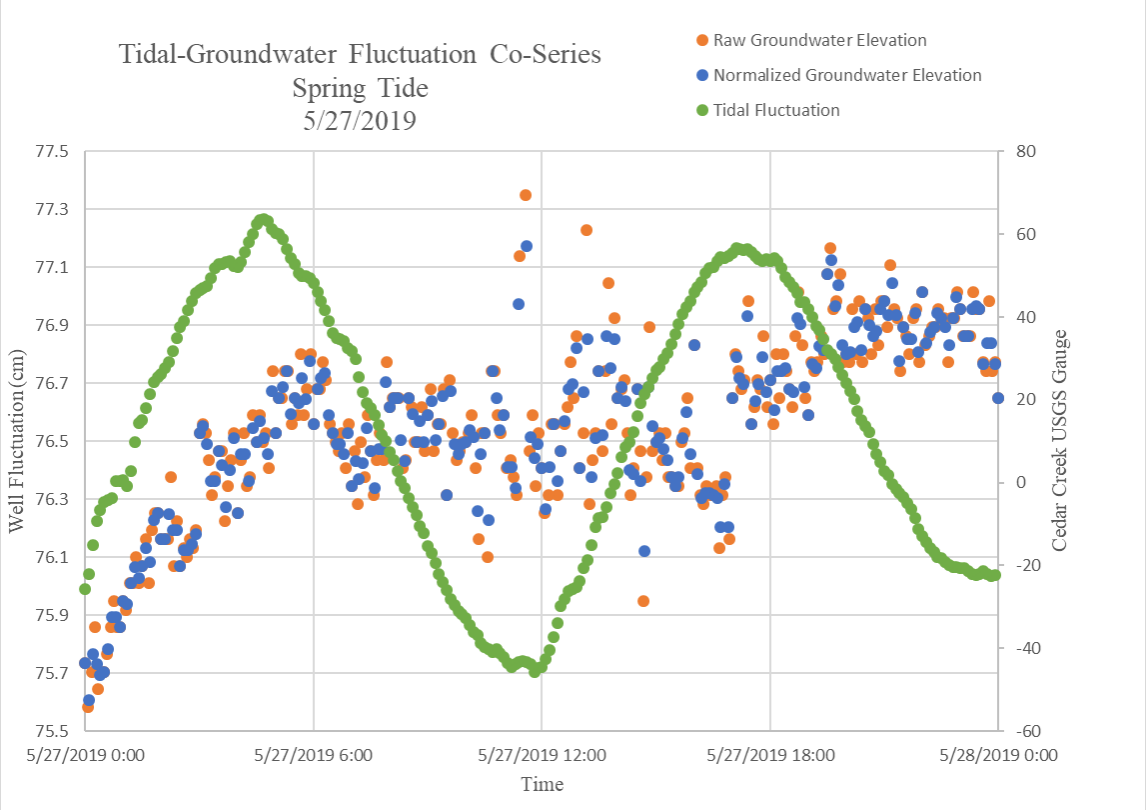

Figure 7: Co-series chart detailing the process to establish a common time base for MW-1D, as well as calculate the values for h_0, h_x, and t_0. Normalized groundwater fluctuation values occur at the same time tidal fluctuation data is recorded.

Salinity sampling

Upon completion of the hydraulic head data collection, groundwater samples were collected using a 2cm diameter bailer. All samples were tested for salinity using a Sybon Opticon Series salinity refractometer. Samples were chilled to ~6.5^{o} C prior to salinity testing. Salinity data was recorded and plotted by well location and distance from Cedar Creek.

Results

Stratigraphy of Slaughter Beach salt marsh

Five major lithostratigraphic units were identified in core logs based on sediment grain size, recognizable plant macro-fossils and position within the sediment column: high marsh peat, low marsh peat, basal peat, tidal mud, and sand. These units were correlated across the study area transect to form a stratigraphic cross section (Figure 8).

The Slaughter Beach tidal sediments are uniformly underlain by a layer of pre-Holocene, fine to medium grain, gray sand. Overlying the sand is a dark brown to black layer of basal peat, that is found at elevations of -2.5m to -5.5m NAVD88. The basal peat was found in all cores with the exception of cores SP-1 and GWSB-2. Low marsh peat sediments, represented by gray brown muddy peat and root stem fragments of *Sp. Alt.,* overlay the basal peat from -2.5m to the surface of the marsh platform toward the Delaware Bay coast. High marsh peat sediments overlay the low marsh peat on the Cedar Creek side of the Slaughter Beach salt marsh. High marsh peat is described as a fibrous peat with fragments of *Sp. Patens*. Finally, interbedded layers of gray mud, that represent open water environments were identified at various depths within the Slaughter Beach salt marsh deposits. These mud units represent tidal flat or tidal

channel depositional environments. Lenses of coarse sands interbedded between low-salt marsh peat found in core GWSB-2 indicate the presence of over-wash storm deposits.

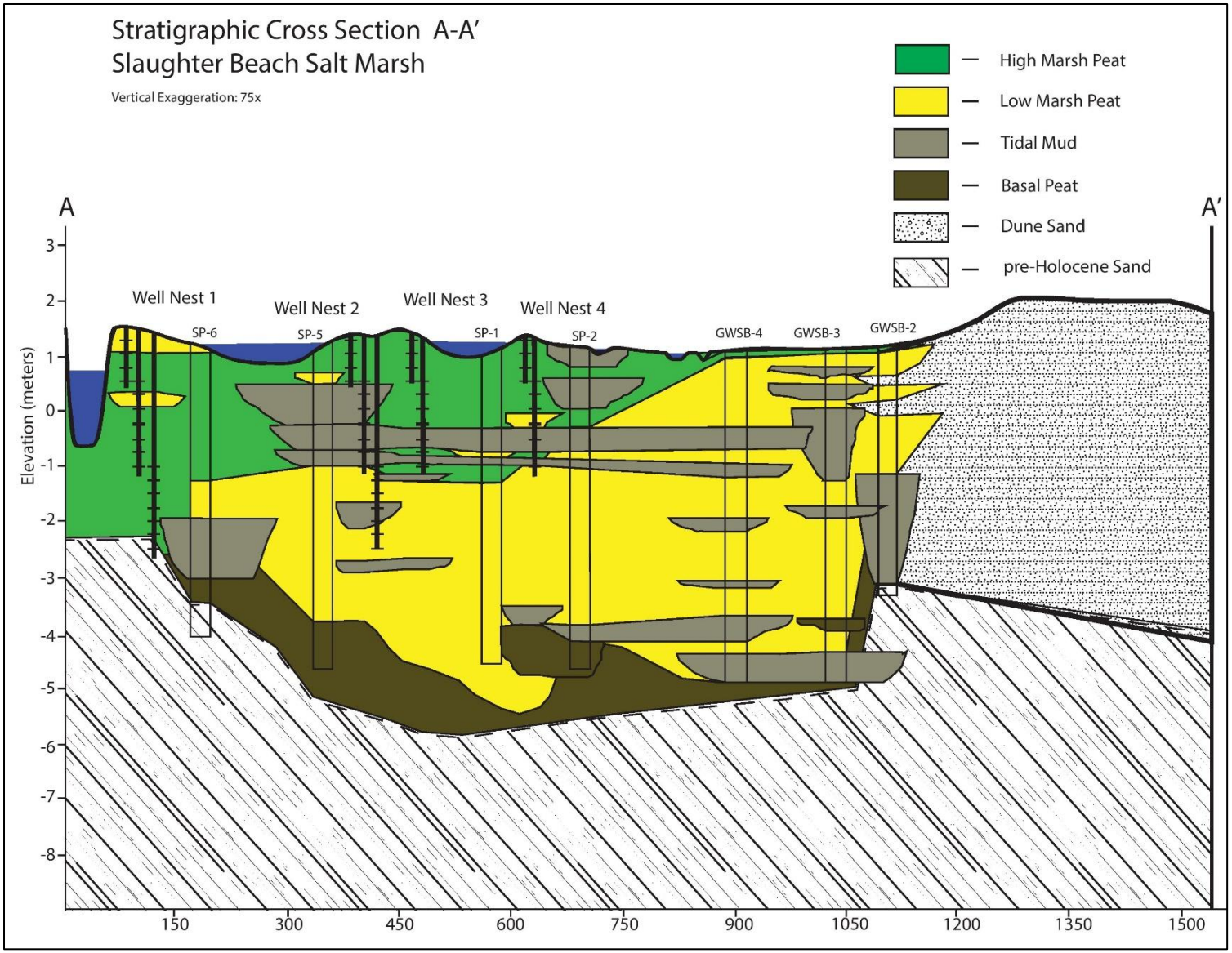

Figure 8: Detailed stratigraphic cross section constructed from core logs taken along the transect A-A'.

Drone Flight Imagery Analysis

Comparison of drone imagery collected at low and high tide documented an increase of the number of ponds from175 ponds at peak low tide to 205 ponds at peak high tide. Conversely, the total surface area of ponds decreased from 25.08% at low tide to 25.07% at peak high tide (Figure 9). Normalized circularity and the range of salt pond area were also calculated (Table 3).

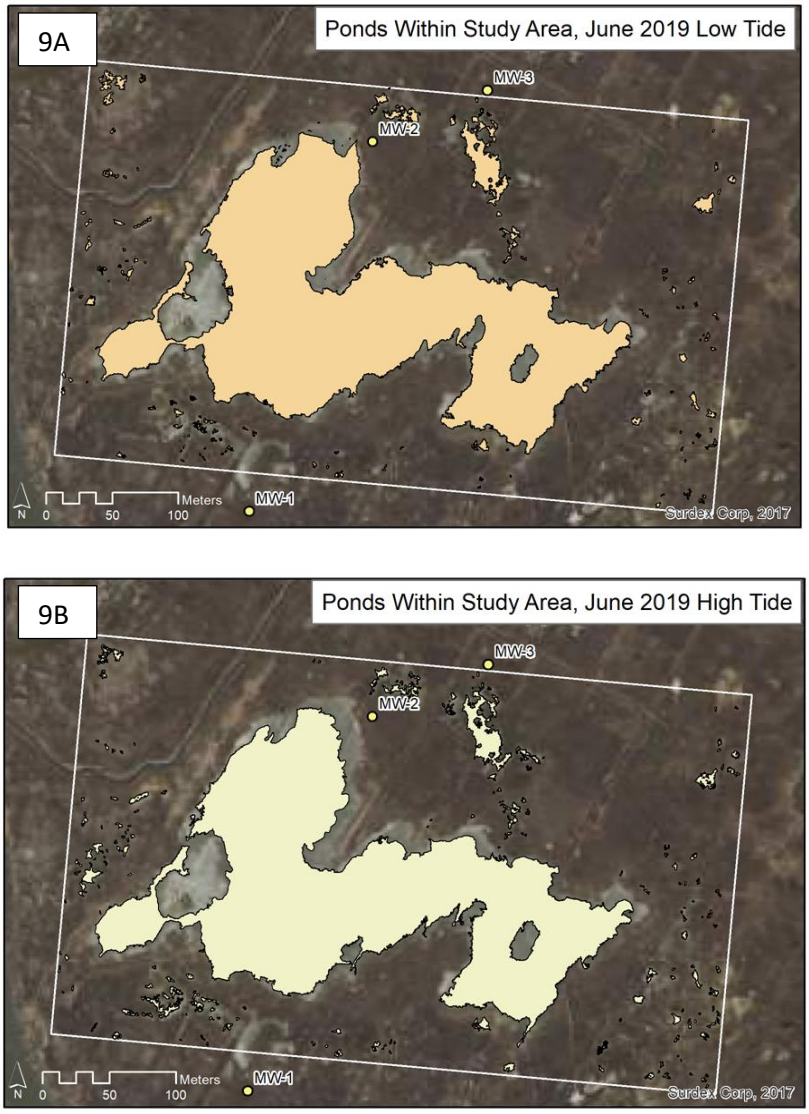

Figure 9: Surface area of 0.15km^2 around the large pond in the study area. Ponds digitized from drone flight imagery collected at low tide (9A) and high tide (9B).

	Total number of ponds	Total surface area of ponds (km^2)	Range of salt pond size (m^2)			Normalized circularity of salt ponds		
			0-10	10-100	100-1000	0-0.33	0.33-0.66	0.66-1
Low Tide	175	0.0387	142	28	4	106	58	11
High Tide	205	0.0376	153	48	3	171	28	6

Table 3: Number of salt ponds and their characteristics documented by imagery analysis of the 0.15km2 study area surrounding the large pond. Data analysis provided by Cameron Knight.

Groundwater and Tidal Fluctuation

Observation well data plotted on a co-series chart revealed cyclic head fluctuation in all of the wells (Figure 10). Hydraulic head in the shallow wells decreased with distance from Cedar Creek with an overall hydraulic gradient of 9.41×10^{-4} from MW-1 to MW-4. The vertical hydraulic gradient was 0.4. Amplitudes of head fluctuation were calculated to follow the tidal cycle (Table 4).

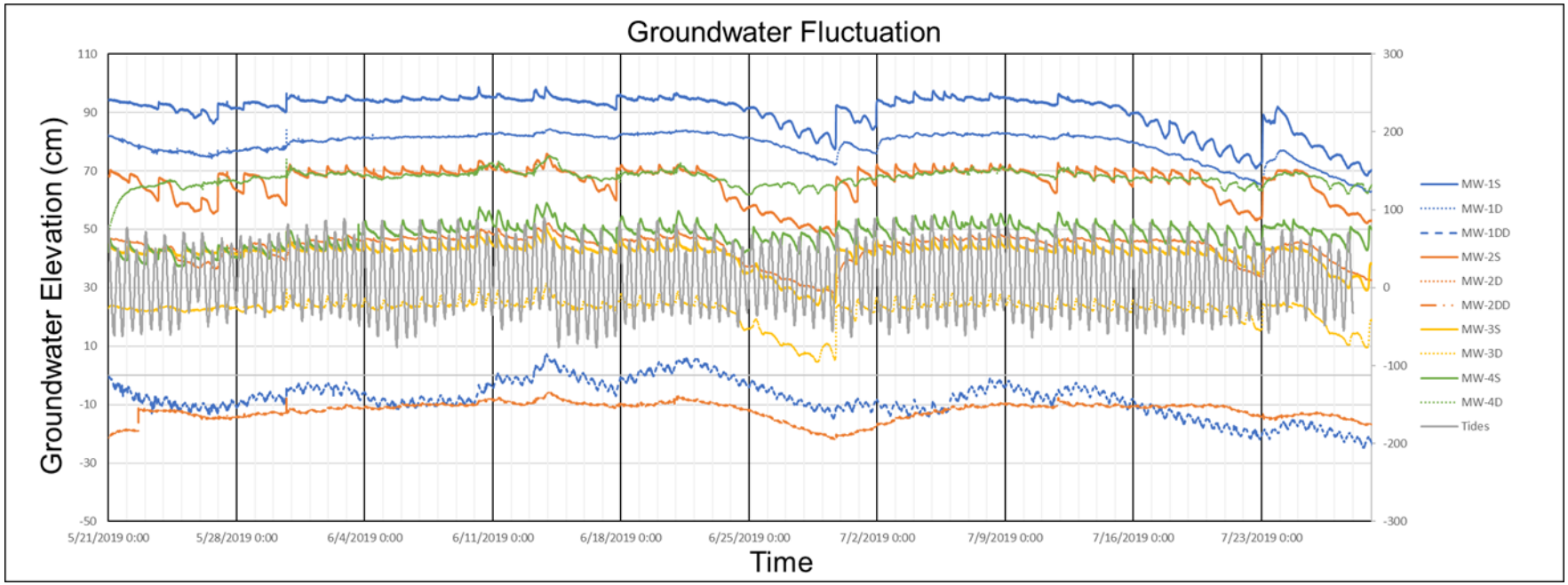

Figure 10: Time series chart depicting hydraulic head in each well along with the stage of Cedar Creek. Well nests are color coded.

	Head at High Tide (cm)	Head at Low Tide (cm)	Tidal Amplitude (cm)
MW-1S	93.10	91.25	1.85
MW-1D	76.80	76.25	0.55
MW-1DD	-9.25	-12.05	2.80
MW-2S	69.00	63.38	5.62
MW-2D	43.71	40.64	3.07
MW-2DD	-14.27	-14.87	0.60
MW-3S	43.63	41.51	2.12
MW-3D	23.90	23.25	0.65
MW-4S	44.45	40.32	4.13
MW-4D	66.90	66.10	0.80

Table 4: Calculated tidal amplitude for each well during the tidal cycle on May 27, 2019.

Tidal data collected from the USGS Stream Gauge 01484235 in Cedar Creek reflected a semidiurnal tidal cycle. Cedar Creek experiences a cycle of two nearly equal high tides and two nearly equal low tides each lunar day with tidal range of 1.4m (Figure 10). The tidal elevation ranged from ~ -50cm NAVD88 to nearly 90cm NAVD88.

Head fluctuations in wells correlated with tide cycles. Groundwater in deep wells (MW-1DD and MW-2DD) responded to both high tides and both low tides during the lunar day.

Hydraulic head in shallow wells (MW-1S, MW-2S, MW-3S, and MW-4S) and intermediate wells (MW-1D, MW-2D, MW-3D, and MW-4D), recorded a similar pattern to each other during the tidal cycle. Hydraulic head increased rapidly in these wells at the highest tide during the day and head continued to fall until the next highest tide the following day.

Values for hydraulic conductivity (K) and hydraulic diffusivity (D), were calculated (Table 5). These values are in a good agreement with other salt marsh groundwater studies (Hughes, 2016). The shallow wells had an instantaneous recharge after purging, and therefore could not be analyzed using the Hvorslev Method.

	Distance from Tidal Source (m)	Diffusivity (m2/day)	Hydraulic Conductivity (m/s)
MW-1S	30	1426.124	1.100×10^{-4}
MW-1D	30	1127.024	1.208×10^{-7}
MW-1DD	30	646.448	1.381×10^{-7}
MW-2S	11	191.735	1.467×10^{-5}
MW-2D	11	177.942	2.490×10^{-7}
MW-2DD	11	176.218	2.531×10^{-7}
MW-3S	19	168.484	1.333×10^{-5}
MW-3D	19	361.144	2.411×10^{-7}
MW-4S	16	240.147	1.867×10^{-5}
MW-4D	16	402.436	5.360×10^{-8}

Table 5: Calculated hydraulic characteristics for each well in the study area. Hydraulic Conductivity for shallow wells was calculated using the tidal method, due to their rapid recharge.

Precipitation Events

The groundwater observation data was compared with precipitation recorded by the Slaughter Beach weather station. During the study period it rained only 10 times (Figure 11). Eight out of ten days had >/= 1.75cm of rainfall recorded. The other two precipitation events were minor, with only < .25cm of rainfall.

Hydraulic head in all but the deepest wells (MW-1DD and MW-2DD) increased in response to precipitation events (Figure 11). Sharp increases in hydraulic head were observed immediately following most precipitation events during the study period (Table 6).

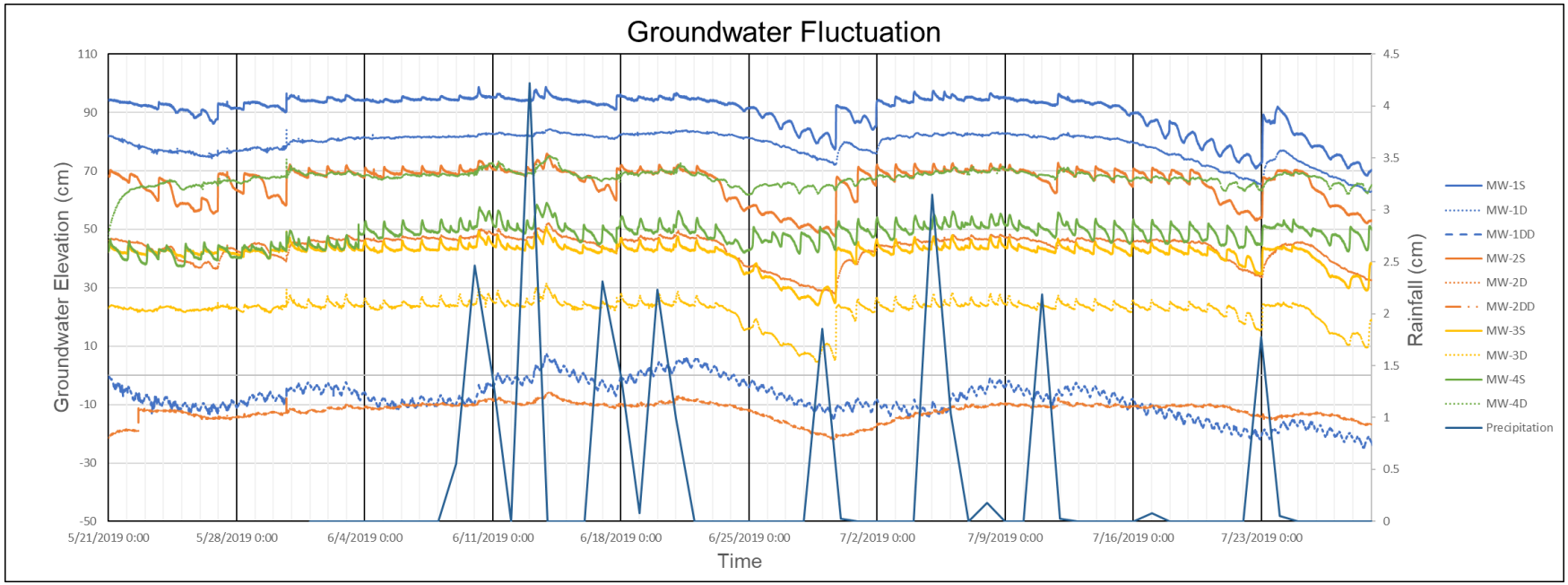

Figure 11: Time series chart depicting well hydraulic head versus Slaughter Beach daily precipitation. Data was not available from May 28 to June 3 due to weather station damage

	Head prior to rainfall (cm)	Head post rainfall (cm)	Head difference (cm)
MW-1S	78	92	14
MW-1D	72	80	8
MW-2S	48	68	20
MW-2D	29	39	10
MW-3S	26	43	17
MW-3D	6	23	17
MW-4S	45	52	7
MW-4D	63	66	3

Table 6: Response in hydraulic head to the rainfall event that occurred on June 29, 2019.

Salinity

Groundwater flowing through the Slaughter Beach salt marsh appeared to be saline with the salinity values ranging between 21ppt and 35ppt. Salinity varied between well locations and depth (Figure 12). Salinity in Well Nest 1 decreased with depth, ranging from 31.5ppt in MW-1S to 26.8ppt in MW-1DD. The highest salinity values were recorded in Well Nest 2, with 34ppt measured in MW-2S, 34.9ppt recorded in MW-2D and 32.9ppt measured in MW-2DD. These values are comparable to the average salinity of ocean water (35ppt) (Manning, 2016). Values recorded in Well Nest 3 are significantly lower with 27ppt measured in MW-3S and 28.6ppt in MW-3D. The lowest salinity values of 22.4ppt and 21.1ppt were recorded in Well Nest 4 (MW-4S and MW-4D).

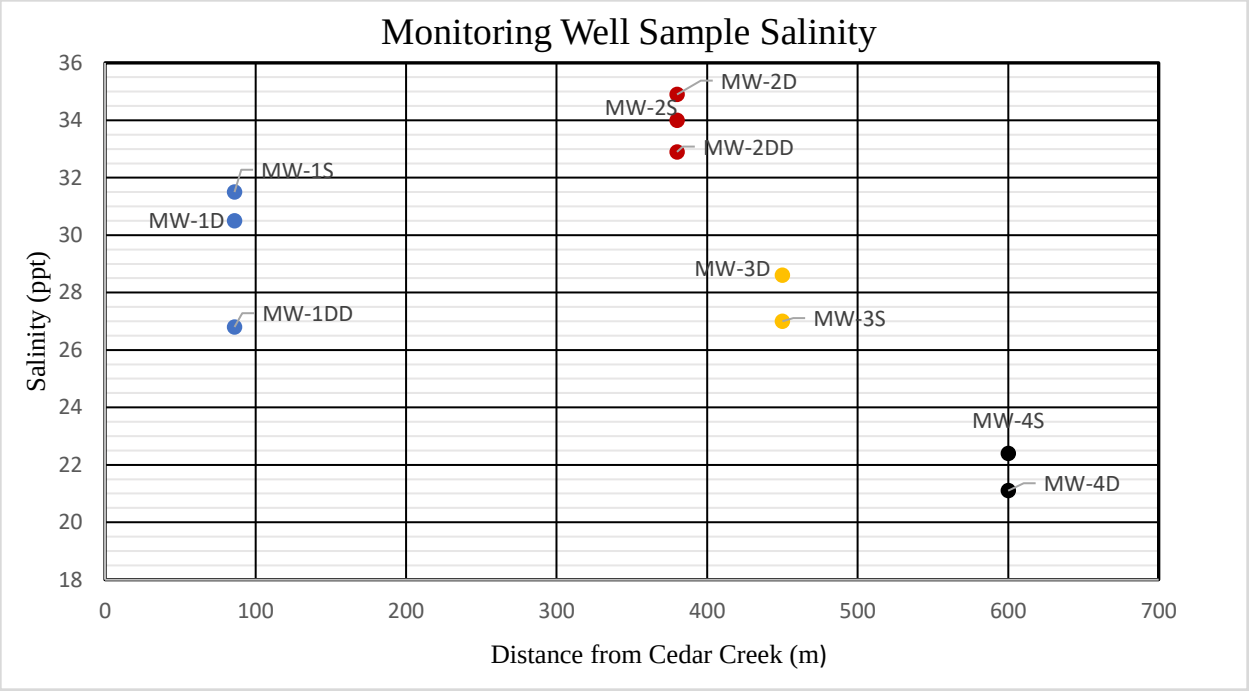

Figure 12: Salinity values for groundwater samples taken from each of the wells. Salinity decreases with distance from Cedar Creek, with the exception of Well Nest 2.

Discussion

Slaughter Beach Stratigraphy

The stratigraphy of the Slaughter Beach salt marsh reveals ~2.5 – 3m thick high marsh sediment deposits onlapping ~4 – 5m thick low marsh deposits. A layer of tidal mud extending across the sequence at the depth of -25cm could possibly act as an aquitard. The aquitard is separating two hydrologic units: an unconfined surficial aquifer recharged by tidal flooding and precipitation and the confined deep aquifer recharged by Cedar Creek and regional groundwater flow from the uplands, which is evident in the lower salinity measured in MW-1DD. Lenses of coarse sands found in core GWSB-4 are most likely over-wash storm deposits.

Tidal Influence on Salt Ponds

While previous studies showed seasonal changes in salt pond morphology (Geyer et al, 2018, Cohen et al., 2019), the drone imagery analysis performed to compare changes of salt pond size during the tidal cycle did not show significant change in the size of the large pond in the Slaughter Beach salt marsh between high tide and low tide. However, the number of ponds within the study area increased between high and low tides.

Hydrologic Characteristics

Studies conducted in coastal marsh ecosystems discovered tidal forcing as the main control of head variation in the mid to high marsh (Hughes, 2016). However, the relationship between salt pond development and groundwater fluctuations were never established. Hydraulic head fluctuations in all monitoring wells in the Slaughter Beach salt marsh show an overall correlation with tidal cycles. However, there are significant differences in groundwater response to tides based on its depth. In the shallow (1m) wells (MW-1S, MW-2S, MW-3S, and MW-4S) changes in hydraulic head corresponded to the highest of the two high tides during each day, rising rapidly and draining slowly until the next highest tide. In the intermediate depth (3m) wells (MW-1D, MW-2D, and MW-3D) hydraulic head displayed minor changes in response to tides. The most noticeable change in hydraulic head in response to tidal influence was recorded in MW-1DD, one of the deepest wells (5m), and the closest to Cedar Creek. We assume that it is directly connected to groundwater flow from Cedar Creek. This also indicates that Cedar Creek is a losing stream, rather than a gaining stream.

Changes in hydraulic head in all but the deepest wells (MW-1DD and MW-2DD) were documented in response to precipitation events (Figure 11). Sharp increases in hydraulic head

was observed immediately following most precipitation events during the study period. Records from the shallow wells documented the greatest increase in head following precipitation, ranging from a head difference of 14cm to 20cm. This supports the hypothesis of 2 existing aquifers, with the shallow aquifer being recharged through semidiurnal tidal flooding and precipitation and the deep aquifer being recharged by regional groundwater flow from the uplands and Cedar Creek.

Calculated values for hydraulic conductivity (K) and hydraulic diffusivity (D), reflected the typical hydrologic characteristics of estuarine marsh soils (Fetter, 2018), which typically range from 10^{-5} m/s to 10^{-9}m/s for hydraulic conductivity (Table 5). The shallow wells had an instantaneous recharge after purging, and therefore were analyzed using the tidal method for diffusivity, rather than the Hvorslev Method for hydraulic conductivity. This suggests that the surficial aquifer is directly connected to surface water on the marsh.

Hydraulic head fluctuation during the tidal cycle did not significantly impact groundwater flow direction. Groundwater elevation decreases in proportion to distance from Cedar Creek and decreases with depth with the exception of the eastern marsh falling in the dune recharge area.

One possible explanation for the upward vertical gradient in Well Nest 4 could be stratigraphic controls. The intermediate (3m) depth well MW-4D penetrates the aquitard layer of tidal mud. The tidal mud consists of fine, low permeability silt and clay; which will restrict groundwater flow. Confining pressure from this lithostratigraphic unit could increase the pressure head within MW-4D.

Hydrogeologic cross sections constructed for the study area reflect an overall downward vertical gradient in hydraulic head (Figure 13). Groundwater flows away from Cedar Creek and

moves towards Delaware Bay in the deep aquifer. Based on groundwater flow patterns, the ponds on the salt marsh surface are losing ponds; water drains from them into the groundwater system of the shallow aquifer, that is underlain by a semi-impermeable silty-clay layer.

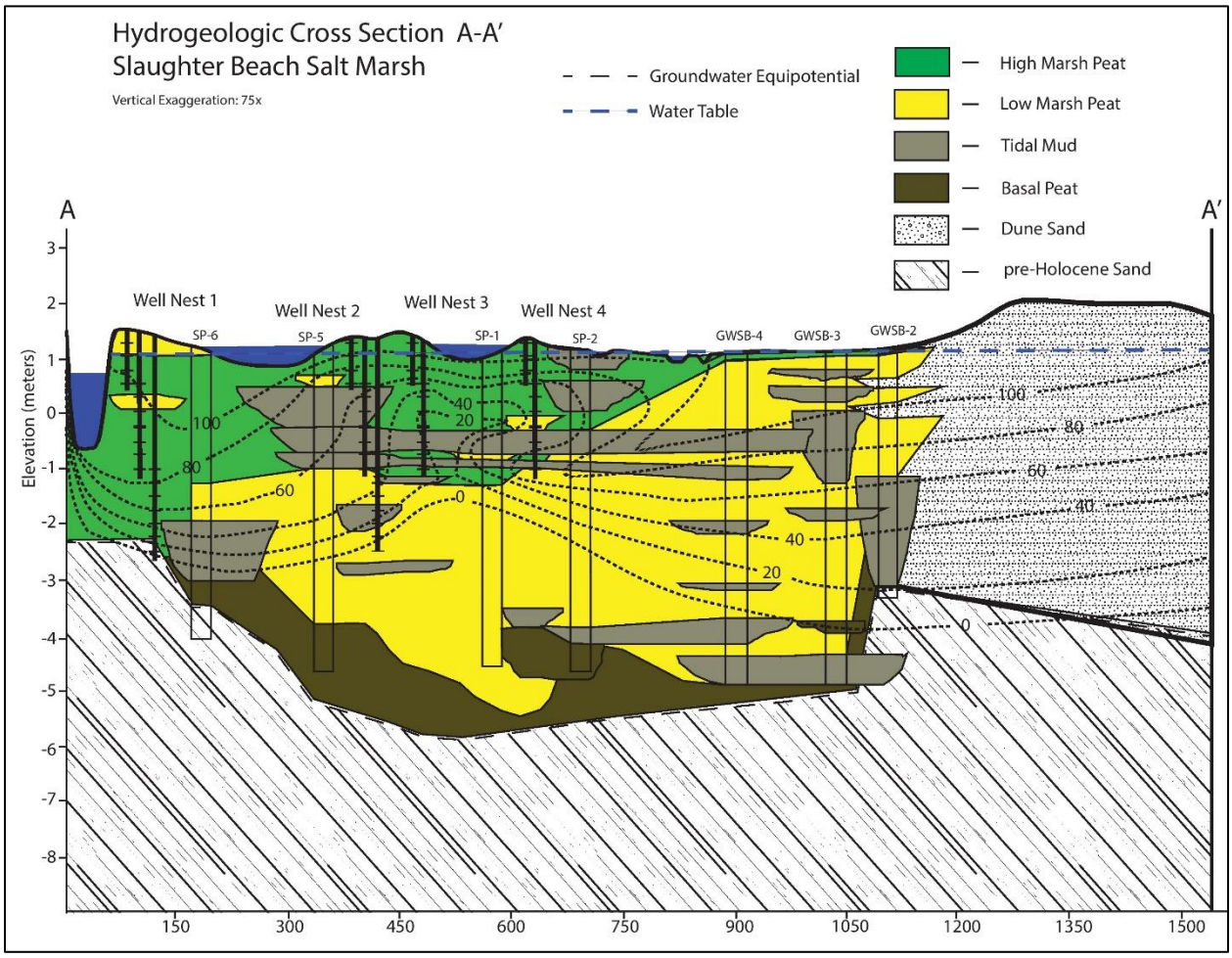

Figure 13: Hydrogeologic cross section of the study area. The spring tide occurring at 9:57 PM on June 3rd, 2019 was used to construct the equipotential lines.

The groundwater flow pattern reflects the presence of two local aquifers: a shallow aquifer, consisting of salt marsh peat units (1-1.5m deep) and a deep aquifer (3-4m deep). The deep aquifer is confined by a 0.5m thick layer of tidal mud and seems to extend into the pre-Holocene sand underlying the Slaughter Beach salt marsh sediment deposits. The shallow aquifer has limited flow due to the tidal mud deposits, which do not readily transmit flow. The deep aquifer is most likely transmitting regional groundwater flow from the headlands and experiencing tidal influence from Cedar Creek, since its' head is changing in proportion to tidal fluctuation. The shallow aquifer is recharged by tidal flooding from the network of shallow tidal creeks and mosquito ditches of the marsh surface and precipitation.

Salinity values from groundwater samples reflect a more saline deep aquifer and a more brackish shallow aquifer. Deep and intermediate wells in the center of the study area (MW-1D, MW-2D, MW-2DD, and MW-3D) have significantly higher salinity values. This is most likely due to direct recharge from Cedar Creek into the deep aquifer as well as groundwater mixing from Delaware Bay. Although MW-1DD penetrates the deep aquifer, it has a lower salinity. This is most likely due to regional freshwater discharge from the headlands mixing with saline water discharged from Cedar Creek, which supports the hypothesis of two separate aquifers. MW-4S and MW-4D recorded the lowest salinity values. The most likely explanation for this would be freshwater run-off from the dune, where precipitation discharges beneath the tidal mud sediments into the aquifer from the dune sands. Although MW-2S was bored into the shallow aquifer, the salinity recorded there is high, probably because of the proximity of two salt ponds and a tidal channel. MW-2 is closer to a tidal channel than any other wells and most likely receives a steady influx of saline water from the surface.

Conclusion

Drone imagery collected from flights at high tide and low tide did not document major change in size of the large pond within the study area, however the number of small ponds (0 – $10m^2$) increased from 142 to 153 during the tidal cycle.

This study documented two local hydrologic units: a shallow unconfined aquifer, and deep confined aquifer that extends into the pre-Holocene sand. The overall direction of groundwater flow in the Slaughter Beach salt marsh is in the northeast direction towards Delaware Bay, with a hydraulic gradient of 9.41×10^{-4} and a vertical gradient of 0.4. The hydrogeologic cross section constructed for the study area indicates that Cedar Creek is a losing stream. Saline water enters the creek from Delaware Bay and floods the marsh through the tidal channel and mosquito ditch network, as well as seeps into the stream banks into the marsh sediments.

The deep aquifer extends from the depth of ~4.5m into the surficial Columbia aquifer of Delaware. The deep aquifer is confined by a 0.5m thick unit of tidal mud that extends throughout the salt marsh platform. The shallow aquifer is approximately 2.5m thick and extends to the tidal mud aquitard sediments, which limit its downward flow.

The salinity of the deep aquifer ranges from 27ppt to 35ppt indicating the connection to regional freshwater flow from the headlands and tidal influence from Cedar Creek. The shallow aquifer salinity ranges from 21ppt to 31ppt, reflecting recharge from freshwater precipitation run-off and tidal flooding from the network of mosquito ditches and tidal channels.

The network of wells monitoring groundwater fluctuation over the period of two full lunar cycles from May 15 to July 27, 2019 at depths of 1m, 3m, and 5m documented that changes in hydraulic head follow the tidal cycles in both aquifers. Comparison of head

fluctuations with precipitation data indicated that the shallow aquifer receives freshwater run-off from the dune while the deep aquifer does not.

Our short-term (2.5 month) study of groundwater flow in combination with drone imagery and stratigraphy has not documented any major salt pond changes, except the response of small ponds to high tide. The salt ponds are developed at the surface of the shallow unconfined aquifer and recharged by tides and precipitation with a limited connection to the deep aquifer. Ponds become fully charged throughout the tidal cycle due to the tidal mud aquitard. Therefore, their changes are related to changes in the volume of tidal flow and hydrologic regime of a shallow tidal drainage network. As sea level continues to rise salt ponds will develop, merge with other ponds and grow in size, reducing the vegetated surface of the salt marsh platform. Rapid development of salt ponds could reduce the marshes ability to accommodate to sea level rise.

This study has established a baseline for quantitative and qualitative analysis of the groundwater hydrology active within the Slaughter Beach salt marsh. Continued monitoring of the site will be necessary to provide understanding of the localized groundwater flow and salt pond morphology in the study area.

References

Barbier, E.B., Hacker, S.D., Kennedy, C., Koch, E.W., Stier, A.C., Silliman, B.R., 2011, The value of estuarine and coastal ecosystem services: Ecological Monographs, v. 81, no. 2, p. 169-193

Beers, D.G., 1868, Atlas of the State of Delaware, Pomeroy and Beers, Philadelphia, 58 p.

Bourn, W.S., Cottam, C., 1950, Some biological effects of ditching tidewater marshes: Fish and Wildlife Service Research Report 19, 16 p.

Cao, M., Xin, P., Guanqiu, J., Ling, L., 2012, A field study on groundwater dynamics in a salt marsh –Chongm Dongtan wetland: Ecological Engineering, v. 40, p. 61-69, doi:10.1016/j.ecoleng.2011.12.018

Cohen, M., 2019, Slaughter Beach salt pond and water channel dynamicism [M.S. Thesis]: West Chester University, 37 p.

Fetter, C.W., 2018, Applied Hydrogeology: Long Grove, Waveland Press, 598 p.

Gardner, L.R., Gaines, E.F., 2008, A method for estimating pore water drainage from marsh soils using rainfall and well records: Estuarine, Coastal and Shelf Science, v. 79, p. 51-58. https://doi.org/10.1016/j.ecss.2008.03.014

Geyer, A., 2018, Geomorphic characterization of salt ponds in Slaughter Beach, Delaware [M.S. Thesis]: West Chester University, 34 p.

Hughes,A.L., 2016, Ecohydrology And Groundwater Dynamics In A Salt Marsh Island: [PhD. Dissertation]: University of South Carolina, 177 p.

Hvorslev, M.J., 1951, Time lag and soil permeability in ground-water observations: U.S. Army Corps of Engineers, Bulletin no. 36, 53 p.

Jacob, C. E. Flow of groundwater, in Engineering Hydraulics, edited by H. Rouse, John Wiley, New York, p. 321-386. 1950

Jiao, J., Post, V., 2019, Coastal Hydrogeology: New York, Cambridge University Press, 475 p.

Kasper, J.W., 2017, Delaware's 2016 305(b) Groundwater-Quality Assessment Based on Public Well Data: Results of Sampling, October 1, 2013 through September 30, 2015: Delaware Department of Natural Resources & Environmental Control, 55p.

Li, H., Jiao, J.J., 2002, Tidal groundwater level fluctuations in L-shaped leaky coastal aquifer system: Journal of Hydrology, v. 268, p. 234 – 243.

Mariotti, G., 2016, Revisiting salt marsh resilience to sea level rise: Are ponds responsible for permanent land loss?: Journal of Geophysical Research: Earth Surface, v. 121, no. 7

Manning, J.C., 2016, Applied Principles of Hydrology, Long Grove, Waveland Press, 276 p.

Mayor, J.R., Hicks, C.E., 2008, Potential Impacts of Elevated CO_2 on Plant Interactions, Sustained Growth, and Carbon Cycling in Salt Marsh Ecosystems, *in* Silliman, B.R., Grosholz, T., Bertness, M.D., eds., Human impacts on salt marshes: a global perspective: University of California Press, p. 207-230.

McKenna, T., 2018, Characterization of Tidal Wetland Inundation in the Murderkill Estuary: Delaware Geological Survey, Report of Investigations, No. 81.

Morgan, P. A., Burdick, D.M., Short, F.T., 2009, The functions and values of fringing salt marshes in Northern New England, USA: Estuaries and Coasts v. 32 p.483–495.

Nelson, J.L., Zavaleta, E.S., 2012, Salt Marsh as a Coastal Filter for the Oceans: Changes in Function with Experimental Increases in Nitrogen Loading and Sea-Level Rise: Public Library of Science ONE, v. 7, p. 1 – 14.

Nikitina, Kemp, Engelhart, Horton, Hill, & Kopp, 2015, Sea-level change and subsidence in the Delaware Estuary during the last ~2200 years. Estuarine, Coastal and Shelf Science, v. 164, p. 506-519.

Ramsey, K.W., 1997, Geology of the Milford and Mispillion River Quadrangles: Delaware Geological Survey, Report of Investigations, No. 55.

Reed, D.J., 1995, The response of coastal marshes to sea-level rise: survival or submergence?: Earth Surface Processes and Landforms, v. 20, no. 1, p. 39-48.

Scharf, J.T., 1888, History of Delaware: 1609 – 1888: Philadelphia, L. J. Richards & Co. 946 p.

Silvestri, S., Defina, A., Marani, M., 2005, Estuarine, Coastal and Shelf Science, v. 62, no. 1-2, p. 119-130. https://doi.org/10.1016/j.ecss.2004.08.010

Smith, E.R., 1988, Case histories of Corps breakwater and Jetty structures: Report 5, North Atlantic Division: Coastal Engineering Research Center; prepared for Department of the Army, US Army Corps of Engineers.

Thibodeau, P.M., Gardner, L.R., Reeves, H.W., 1998, The role of groundwater flow in controlling the spatial distribution of soil salinity and rooted macrophytes in a southeastern salt marsh, USA: Mangroves and Salt Marshes, v. 2, p. 1-13

Townend, I., Fletcher, C., Knappen, M., Rossington, K., 2011 A review of salt marsh dynamics, Water and Environment Journal, v. 25, p. 477-488.

Wilson, A.M., Moore, W.S., Joye, S.B., Anderson, J.L., Schutte, C.A., 2011, Storm-driven groundwater flow in a salt marsh: Water Resources Research, v. 47, W02535, doi:10.1029/2010WR009496.

Wilson, K.R., Kelley, J.T., Croitoru, A., Dionne, M., Belknap, D.F., Steneck, R., 2009, Stratigraphic and Ecophysical Characterizations of Salt Pools: Dynamic Landforms of the Webhannet Salt Marsh, Wells, ME, USA: Estuaries and Coasts, v. 32, p. 855-870

Appendix A: Hvorslev Drawdown Curves

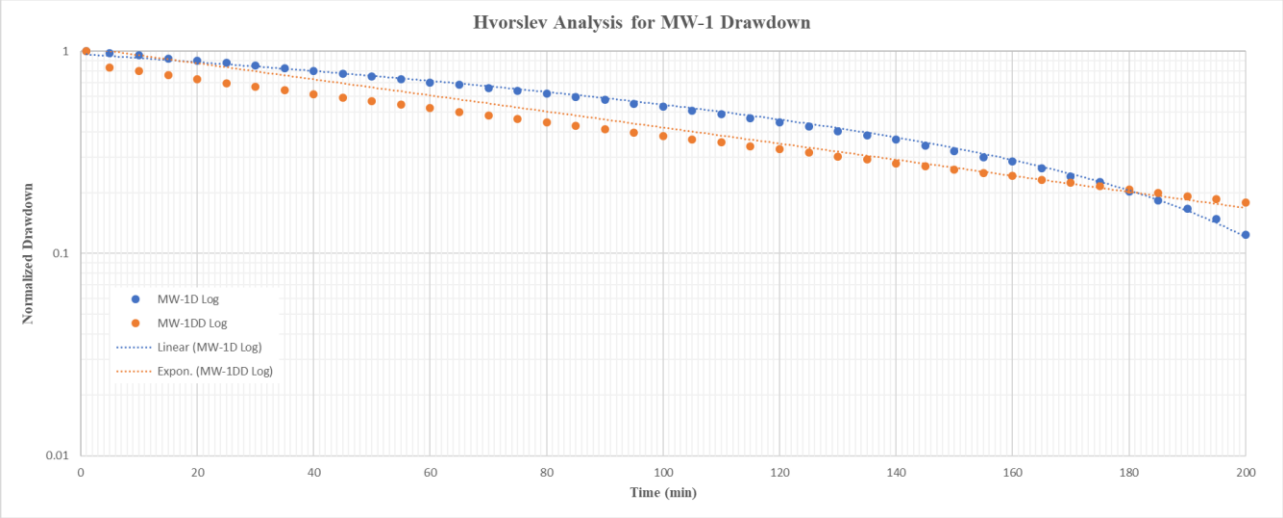

Figure 14: Hvorslev drawdown curve for MW-1D and MW-1DD

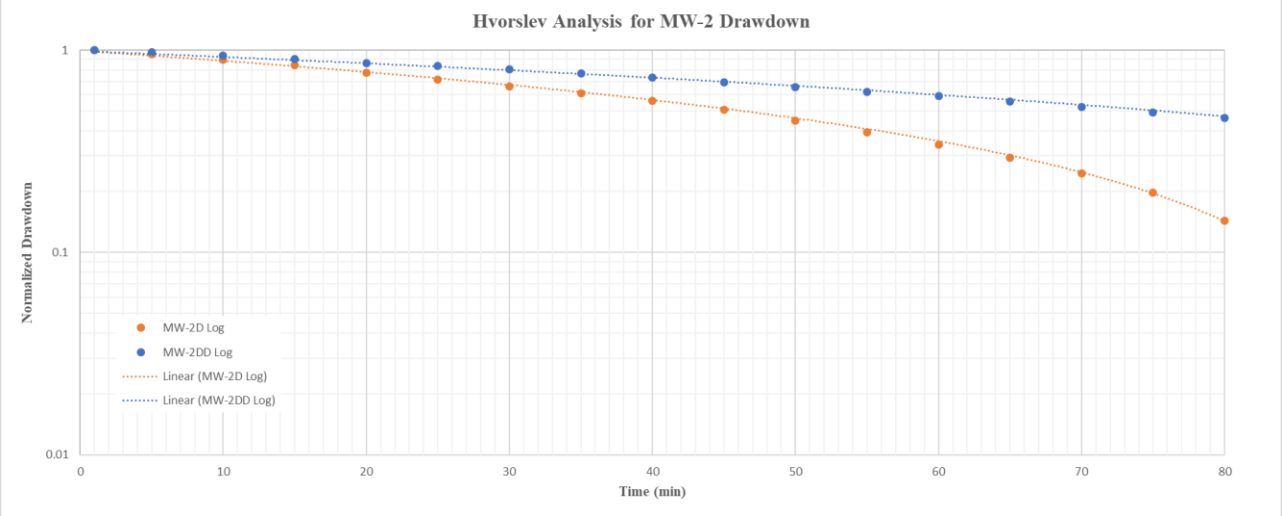

Figure 15: Hvorslev drawdown curve for MW-2D and MW-2DD.

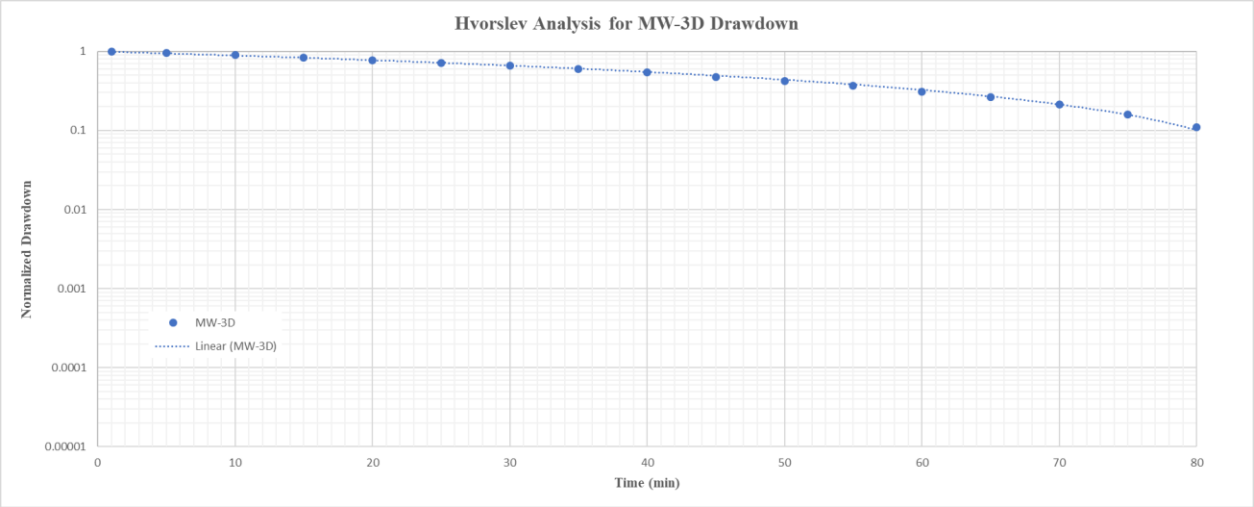

Figure 16: Hvorslev drawdown curve for MW-3D.

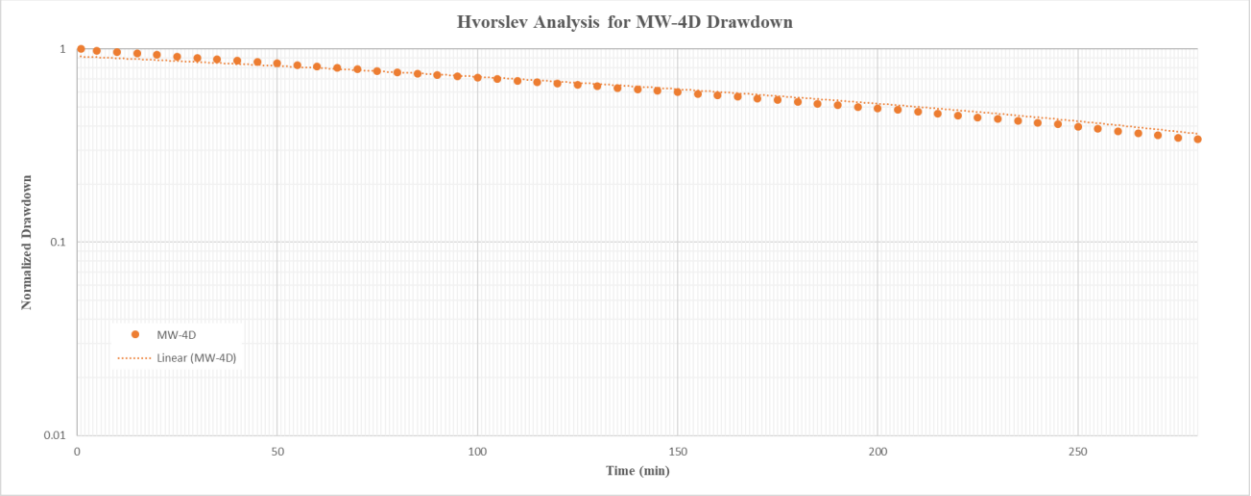

Figure 17: Hvorslev drawdown curve for MW-4D.